

Linseed Oil Nanoemulsion with Pluronic® F127 Loaded with Betulinic Acid: Preparation, Rheology, MTT Assay and *in vitro* Release Kinetics

Louhana M. Rebouças,^a Alexandre C. C. Sousa,^a Nilce V. Gramosa,^a
Tamara G. de Araújo,^b Fátima de Cássia E. de Oliveira,^c Cláudia do Ó Pessoa,^c
Rinaldo S. Araújo,^d Emília M. A. Santos^d and Nágila M. P. S. Ricardo^{✉*,a}

^aDepartamento de Química Orgânica e Inorgânica, Centro de Ciências,
Universidade Federal do Ceará, 60440-900 Fortaleza-CE, Brazil

^bDepartamento de Farmácia, Universidade Federal do Ceará (UFC),
Campus do Porangabuçu, 60430-170 Fortaleza-CE, Brazil

^cDepartamento Fisiologia e Farmacologia, Universidade Federal do Ceará,
Campus do Porangabuçu, 60431-970 Fortaleza-CE, Brazil

^dDepartamento de Química e Meio Ambiente,
Instituto Federal de Educação Ciência e Tecnologia do Ceará,
60040-215 Fortaleza-CE, Brazil

The main objective of this work was to develop a nanoemulsion based on linseed oil and betulinic acid, stabilized with Pluronic F127 and polyglycerol polyricinoleate, for anticancer applications. The nanoemulsions were synthesized by ultrasound and evaluated for *in vitro* cytotoxicity, particle size, polydispersity index, zeta potential, morphology, encapsulation efficiency, storage stability, rheology and *in vitro* release kinetics. *In vitro* cytotoxicity assays were performed by 3-(4,5-dimethylthiazol-2-yl)-2,5-diphenyltetrazolium bromide (MTT) assay (72 h) against HCT-116 (colorectal carcinoma), SNB-19 (glioblastoma), NCI-H460 (lung carcinoma) and L-929 (normal fibroblasts) cells. The determination of 50% inhibitory concentration (IC₅₀) showed an increased selectivity for the emulsified betulinic acid when compared to its free form for the HCT-116 cells. The IC₅₀ values for the synthesized nanoemulsions showed a range from 3.2 to 3.7 μM (HCT-116), 5.6 and 11.5 μM (NCI-H460), 5.8 and 7.3 μM (SNB-19) and > 16.5 μM for normal fibroblasts. In the 48 h *in vitro* release assays, it presented controlled release explained by the Korsmeyer-Peppas model, releasing 572.25 and 619.95 μg of betulinic acid in a controlled way, generating promising perspectives for the prolonged release of betulinic acid in anticancer applications.

Keywords: betulinic acid, MTT assay, nanoemulsion, pluronic F127, linseed oil

Introduction

Versatile applications of nanoemulsions in pharmacology and healthcare sectors are an increasing field of study.¹ For instance, disulfiram (DSF) loaded nanoemulsion have been delivered intranasally to the rat brains for glioblastoma treatment.² Gel-in-water nanoemulsions have been developed aiming to increase the delivery of hydrophobic drugs via encapsulation.³ Self-nanoemulsifying drug delivery systems have improved the solubility on the

in vitro release of anticancer drugs, as well as the *ex-vivo* permeation and anticancer activity.^{4,5} Additionally, nanoemulsions can be utilized for topical delivery, generating anti-inflammatory, anesthetic, antifungal, antioxidant and anticarcinogenic activity.⁶

Betulinic acid [(3β)-3-hydroxy-lup-20(29)-en-28-oic acid] presents anticancer activity with selective action reported by Pisha *et al.*,⁷ being considered a viable therapeutic option for advanced melanoma cells,⁸ inducing them to *in vitro* and *in vivo* apoptosis.^{8,9} This compound is a pentacyclic triterpene that can be extracted from the outermost layer bark of the *Betula alba* L. The anticancer activity of BA (betulinic acid) also has been confirmed for breast, colon, lung, pancreas, ovary, neuroblastoma

*e-mail: naricard@ufc.br

Editor handled this article: Fernando C. Giacomelli (Associate)

or osteosarcoma cell lines.¹⁰⁻¹² However, its poor aqueous solubility limits its delivery in medicines.

In order to increase the delivery of low solubility compounds, nanoemulsions have been used in the development of new strategies. Nanoemulsions are oil-in-water or water-in-oil dispersions with droplets in the range from 20 to 500 nm, formed by a dispersed phase into a continuous phase, stabilized with the use of surfactants.¹³ Thus, oil droplets allow the encapsulation of hydrophobic bioactives in an oil-in-water nanoemulsion, representing a drug nanocarrier with high encapsulation efficiency and high stability that can increase the drug bioavailability.

In the present study, the oil from linseed (*Linum usitatissimum* L.) was used. This oil is rich in omega fatty acids (approximately 57% ω 3, 16% ω 6, 18% ω 9), which has beneficial effects, associated with its high lignan content, specifically secolariciresinol diglucoside (SDG).¹⁴ Its use is due to studies that have demonstrated its effect on cell membrane fluidity, showing high influence by the presence of omega-3 or omega-6 fatty acids, which can significantly affect the cellular functions and improve the input of drugs into the cell.¹⁵

Pluronic® F127 (nominal formula $E_{98}P_{67}E_{98}$) is a triblock copolymer where E = oxyethylene, OCH_2CH_2 , P = oxypropylene, $OCH_2CH(CH_3)$, that has been used as surfactant in this study. The advantages of this surfactant consist in its non-toxicity and its increased time of blood circulation, due to the fact that particles formed with this copolymer are not captured by macrophages.^{16,17} Another striking feature of Pluronics is that they have the ability to act as an inhibitor of the glycoprotein P, which is the main membrane protein responsible for the efflux of drugs from the cell. They also act in the cytochrome P450 3A (CYP3A), the main metabolic enzyme of the cell. Thus, Pluronic® F127 was chosen for this study for providing greater availability and less resistance to the drug entrance in the cell, improving perspectives for therapeutic applications.¹⁸

Previous studies report linseed oil-based nanoemulsions using egg phosphatidylcholine as a surfactant, showing to be inhibitors of the angiogenesis process.¹⁹ There are also reports of nanoemulsions using medium-chain fatty acids as an oil phase and lecithin as a surfactant, which have shown to inhibit skin cancer in mice.²⁰

This work reports the development of a nanoemulsion loaded with betulinic acid based on linseed oil, stabilized with Pluronic® F127 and polyglycerol polyricinoleate (PGPR) for controlled release. Additionally, a preliminary assessment of *in vitro* antiproliferative activity against three human tumor cell lines was performed. The prepared nanoemulsions showed an increase in the selectivity of

betulinic acid in relation to the pure active, not showing to be cytotoxic in non-tumor cells at the concentrations tested.

Experimental

Materials

Linseed oil was purchased from Jasmine Alimentos (Paraná, Brazil). Betulinic acid (98% betulinic acid content) was purchased from Xi'an Quanao Biotech Co. Ltd. (Xian, China). Polyglycerol polyricinoleate (PGPR, molecular weight 390.6 Da, PGPR content 98%) was provided by Danisco® (Grindsted, Denmark). Polyoxyethylene-polyoxypropylene block copolymer (Pluronic® F127, molecular weight 12.5 kDa, 99% Pluronic F127 content) and 3-(4,5-dimethylthiazol-2-yl)-2,5-diphenyltetrazolium bromide (MTT reagent) were purchased from Sigma-Aldrich® (St. Louis, USA). Analytical grade chloroform and dimethyl sulfoxide (DMSO) were purchased from LabSynth® (São Paulo, Brazil). Acetonitrile and methanol (high-performance liquid chromatography grade) were purchased from Tedia® (Ohio, USA). Deionized water was obtained from a Milli-Q water purification system Millipore® Corporation (Watford, UK).

Cell lines and culture

The human tumor cell lines used in this study, HCT-116 (colorectal), SNB-19 (glioblastoma) and NCI-H460 (lung), were provided by the National Cancer Institute (NCI, USA). L929 (non-cancerous murine fibroblast) were provided by BCRJ (Banco de Células do Rio de Janeiro). Both have grown in their respective culture media, Roswell Park Memorial Institute (RPMI) 1640 or Dulbecco's Modified Eagle Medium (DMEM, Gibco®), supplemented with 10% fetal bovine serum (Gibco®) and 1% antibiotics (Sigma-Aldrich Co, St. Louis, MO, USA), incubated under 5% of CO_2 .

Linseed oil GC-MS and GC-FID analysis

The fatty acid profile was obtained by gas chromatography coupled to a mass spectrometry (GC-MS) using an Agilent 5977A gas chromatograph (Santa Clara, USA, Agilent Technologies) and the relative percentage by chromatography coupled to a flame ionization detector (GC-FID) using a Shimadzu GC-2010 Plus gas chromatograph (Kyoto, Japan, Shimadzu Corporation). The samples were analyzed on an Agilent 5977A equipped with a HP-5MS fused silica capillary column Agilent (30 m \times 0.25 mm \times 0.25 μ m) connected to a quadrupole detector, operating in the mode EI (electron ionization) at 70 eV and a sampling rate of

2.7 scans s⁻¹. A split ratio of 1:100 was used with 1 µL injection. Helium was used as carrier gas at 1 mL min⁻¹. The injector and interface temperatures were 250 and 280 °C, respectively. The temperature ramp was set initially to 35 °C with consecutive increase to 180 °C at 15 °C min⁻¹, followed by increase to 250 °C at 5 °C min⁻¹. The final temperature was maintained for 23 min. Peaks were identified based on the fragmentation patterns using the NIST Mass Spectral Research Program.²¹ To obtain the relative percentage, the samples were injected into a Shimadzu CG-2010 Plus gas chromatograph equipped with a flame ionization detector (GC-FID) and an RTX-5 methylpolysiloxane column (30 m × 0.25 mm × 0.25 µm). The same method was used for GC-MS.

Synthesis of nanoemulsions

Two formulations denominated FF (only Pluronic F127 as surfactant) and FP (Pluronic F127 and PGPR as surfactant) were prepared according to the composition shown in Table 1.

The betulinic acid was solubilized in 4 mL of chloroform. Then, this solution was added to the linseed oil, homogenized and rotoevaporated at 40 °C, under reduced pressure until the chloroform was completely removed. Subsequently, for FP formulation, the PGPR and the aqueous solution containing Pluronic F127 were added to the oil phase and water, while for formulation FF, only Pluronic F127 and water were added. The formulations were then sonicated on a Branson Sonifier W-450D (Hielscher, Teltow, Germany) with probe, amplitude of 70% and 100-105 W power, for 2 min in 12 cycles of 10 s on and 10 s off, into an ice bath.

HPLC analysis

The quantification of betulinic acid was performed by high-performance liquid chromatography (HPLC).²² Standards of betulinic acid and nanoemulsion samples were analyzed by HPLC Shimadzu CTO-20A (Shimadzu Corporation, Kyoto, Japan) equipped with an ultraviolet detector (UV) at 210 nm. A C-18 column

(4.6 × 250 mm × 5 µm) equipped with automatic temperature (± 0.1 °C) controller module and a mobile phase in the isocratic mode of acetonitrile:methanol (80:20 v/v), with a flow rate of 0.5 mL min⁻¹ were used. The column temperature was maintained at 35.0 ± 0.1 °C.

Particle size and zeta potential

The size of the nanoparticles, estimated by the average hydrodynamic diameter, the polydispersity index (PDI) and the zeta potential (ζ), were determined by dynamic light scattering (DLS) using a NanoZS® (Malvern Instruments, Worcestershire, UK). Measurements were taken at an angle of 90° after dispersion of 50 µL of the nanoemulsions in 5.0 mL of Milli-Q water. All measures were performed in triplicate at 25 °C with comparable conductivity to determine the zeta potential.

Transmission electron microscopy (TEM)

The morphology of the nanoemulsions was observed by transmission electron microscopy TEM JEOL JEM 1101 (Tokyo, Japan, Jeol Corporation) at 40 kV. A droplet was placed on a Formvar carbon-coated copper grid, 200 mesh, and stained with 50 µL of 2% phosphotungstic acid.²³ The stained sample was allowed to dry at room temperature for 10 min.

Encapsulation efficiency

Encapsulation efficiency (EE) was obtained from an ultrafiltration tube Turbo 15 Vivaspin (Sartorius, Gottingen, Germany) 4000 rpm for 30 min, with cut of 3000 Daltons. Thus, the betulinic acid encapsulation efficiency was determined by the difference between the initial amount of bioactive added to the nanoemulsion formulation and the free amount observed after the filtration process, calculated according to the following equation.²⁴

$$EE (\%) = \frac{[BA(t) - BA(ne)]}{BA(t)} \times 100 \quad (1)$$

Table 1. Composition of the formulations

Formulation	HLB	Betulinic acid / mg	Linseed oil / g	PGPR / g	Pluronic F127 / g	Water / g
FF	22	15.3	1.5	–	0.10	8.4
FP	11.5	15.3	1.5	0.05	0.05	8.4
Control-FF	22	–	1.5	–	0.10	8.4
Control-FP	11.5	–	1.5	0.05	0.05	8.4

FF: nanoemulsion with only Pluronic F127 as surfactant; FP: nanoemulsion with Pluronic F127 and PGPR as surfactant; Control-FF: nanoemulsion FF betulinic acid free; Control-FP: nanoemulsion FP betulinic acid free; PGPR: polyglycerol polyricinoleato; HLB: hydrophilic-lipophilic balance.

where, EE (%): encapsulation efficiency, BA(ne): concentration of the non-entrapped betulinic acid, BA(t): total concentration of the betulinic acid in the nanoemulsion.

Rheological assay

The rheological properties of nanoemulsions were determined using cone and plate geometries (40 mm in diameter; 1° cone angle and 27 µm gap at 25 °C) in AR 2000 rheometer (TA Instruments, New Castle, USA), the software used was Rheology Advantage Instrument Control AR.²⁵ The power law was applied to determine the type of fluid using the equation:

$$\tau = K\dot{\gamma}^f \quad (2)$$

where τ is the shear stress, $\dot{\gamma}$ is the shear rate, K is the index of consistency and f is the flow index.²⁶

Storage stability and thermodynamic stability studies

The nanoemulsions were subjected to various conditions of time and temperature to investigate the impact of these conditions on the physical and chemical characteristics. The nanoemulsions were stored at 25 and 45 °C for 90 days, and the average drop diameter, pH, zeta potential and percentage of initial betulinic acid concentration of the nanoemulsions were periodically evaluated to investigate the impact of these conditions on the storage stability of nanoemulsions.

In the thermodynamic stability study, FF and FP nanoemulsions containing betulinic acid were evaluated by three heating-cooling cycles at 45 and 4 °C for 48 h and monitored for any change in appearance, including color change, precipitation and phase separation. Afterwards, the nanoemulsions were centrifuged at a speed of 3500 rpm for 30 min to identify phase separation or precipitation. Finally, the freeze-thaw cycle was performed six times with alternating freeze-thaw cycles at -20 and 25 °C for 24 h in deep freezer and room temperature, respectively, to check for any changes in appearance, including separation of phases, precipitation and color change.²⁷

Measurement of drug solubilities in release mediums

Initially, a solubility test was performed to determine the sink condition for the *in vitro* release study. An excess amount of betulinic acid was added to tubes containing 3 mL of the release mediums DMSO:phosphate buffered (PBS, pH = 7.4) in the ratios 10:90 and 30:70.²⁸ The suspensions were stirred for 72 h at room temperature,

then filtered through a 0.45 µm membrane and diluted for HPLC assay. Previously, unsuccessful attempts have been made to solubilize betulinic acid in buffered phosphate (PBS, pH = 7.4) and alcoholic solutions (10-30%) of this buffer. The sink condition considered is the maximum drug concentration less than 1/3 of the solubility in the release medium.²⁹

In vitro release and kinetic studies

The studies of betulinic acid release from nanoemulsions were carried out in Franz-type diffusion cells under sink condition. In this study, a dialysis membrane (molecular weight cut-off 12-14 kDa, Sigma-Aldrich, St. Louis, USA) was used as a diffusion membrane, which was immersed in the receptor medium for 24 h before the experiment. The diffusion area was 1.55 cm², the receptor compartment was filled with the volume of 11.7 mL of DMSO/phosphate-buffered PBS medium pH = 7.4 30:70 and was magnetically stirred at 200 rpm. Nanoemulsions (1 mL) were placed in the donor compartment. The temperature was maintained at 37.0 ± 0.5 °C for 48 h. To quantify the betulinic acid released, 1 mL samples were removed from the receptor compartment at predetermined time intervals for quantification by HPLC and the same volume removed was replaced with fresh receptor medium. The study was carried out in triplicate for each formulation and for free betulinic acid.

For the kinetic study of release, two mathematical models were applied to the release data obtained separately: the Korsmeyer-Peppas model (equation 3) and the Higuchi model (equation 4).^{30,31}

$$\frac{M_t}{M_\infty} = k_1 t^n \quad (3)$$

where M_t is the drug mass released at time t; M_∞ is the total drug mass; k_1 is a constant related to the structural and geometric characteristics of the dosage form; n is the release exponent indicating the release mechanism.

$$Q = K_h t^{\frac{1}{2}} \quad (4)$$

where Q is cumulative amount of drug released in time t per unit area; K_h is Higuchi dissolution constant.

The models mentioned are applicable to particles formed by polymeric encapsulating materials, such as Pluronic F127 and PGPR used in the formulations. For the applied models, only the points of the first 12 h of release were used (≤ 60% of the total released). The steady state flux of betulinic acid was calculated of the slope of the linear section of the cumulative amount of released (µg cm⁻²)

against time profiles (hours) and lag times were determined as the intercept of steady state flux J to the time axis.³²

MTT assay

The cytotoxic potential for the betulinic acid and nanoemulsions were determined using the 3-(4,5-dimethylthiazol-2-yl)-2,5-diphenyltetrazolium-bromide (MTT) assay.³³ Cells were seeded at concentrations of 0.7×10^5 cells mL^{-1} for HCT-116 (colorectal carcinoma) and L-929 (non-tumor fibroblast) at 7×10^4 cells mL^{-1} and cultivated for 72 h at 37 °C and CO₂ (5%). Betulinic acid, nanoemulsions based betulinic acid and free betulinic acid nanoemulsions were added at various concentrations (0.39-7.00 $\mu\text{g mL}^{-1}$). After the exposure, the medium was changed followed by the addition of 5 μL of MTT reagent (5 mg mL^{-1} stock). The cells were incubated for 3 h at cell culture condition and lysed in DMSO (100 μL *per well*). The absorbance was measured spectrophotometrically using Elisa microplate spectrophotometer (Bio-Rad Laboratories, Hercules, USA) at 570 nm. All absorbance values were corrected against blank wells. The cell viability was calculated by the following formula (A = absorbance):

$$\text{Cell viability (\%)} = \frac{(A_{\text{sample}} - A_{\text{blank}})}{(A_{\text{control}} - A_{\text{blank}})} \times 100 \quad (5)$$

IC₅₀ (half maximal inhibitory concentration) was calculated by using graphical method and linear regression.

Statistical analysis

The statistical evaluations of results were analyzed by GraphPad Prism 5.0.³⁴ The IC₅₀ values are expressed as mean \pm standard deviation (SD). For comparison of several groups, one-way analysis of variance (ANOVA) was applied. For all cytotoxicity analyzes and stability study, $p < 0.05$ was considered statistically significant.

Results and Discussion

Nanoemulsions analysis

Quantitative analyzed linseed oil was made by GC-MS and GC-FID. The major components found were methyl linolenate ($74.16 \pm 0.62\%$), methyl linoleate ($13.62 \pm 0.28\%$), methyl palmitate ($4.84 \pm 0.07\%$), and methyl stearate ($4.12 \pm 0.05\%$). These components were found at 22.63, 22.43, 19.37 and 22.87 min, respectively. The main fatty acid found was linolenic acid (18:3). Thus, these data are close to the values found by Chauhan *et al.*,³⁵ which found 73%

of linolenic acid, 12% of linoleic, 7% of palmitic and 6% of stearic acid, also using a reverse phase column.

The FF and FP nanoemulsions did not show phase separation characteristics, neither creaming nor precipitation as shown in Figures 1a and 1b.

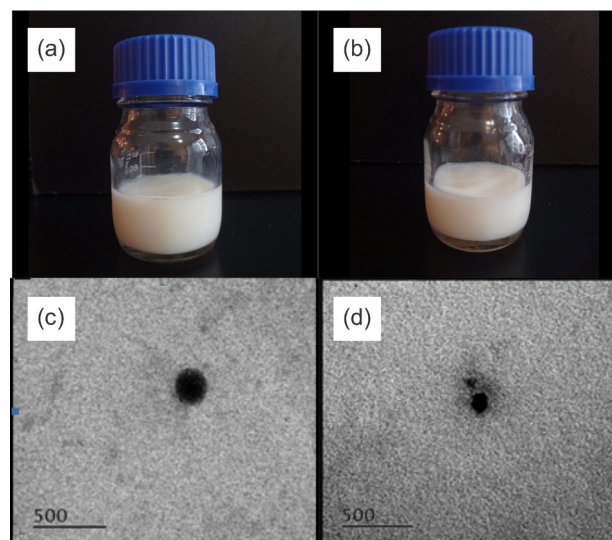


Figure 1. FF and FP nanoemulsion and microscopy. (a) and (c) FF nanoemulsion; (b) and (d) FP nanoemulsion. Scale: 500 nm.

The micrograph of the FF nanoemulsion showed spherical droplets in the nanometer range of approximately 260 nm and this value is close to that obtained by DLS. However, the micrograph of the FP nanoemulsion did not show perfectly spherical droplets, only droplets with irregular borders, with a diameter of approximately 160 nm and with droplets close to each other. This observation may be related to the presence of PGPR and some phenomenon of crystallization of the active in the oil phase as shown in Figures 1c and 1d.

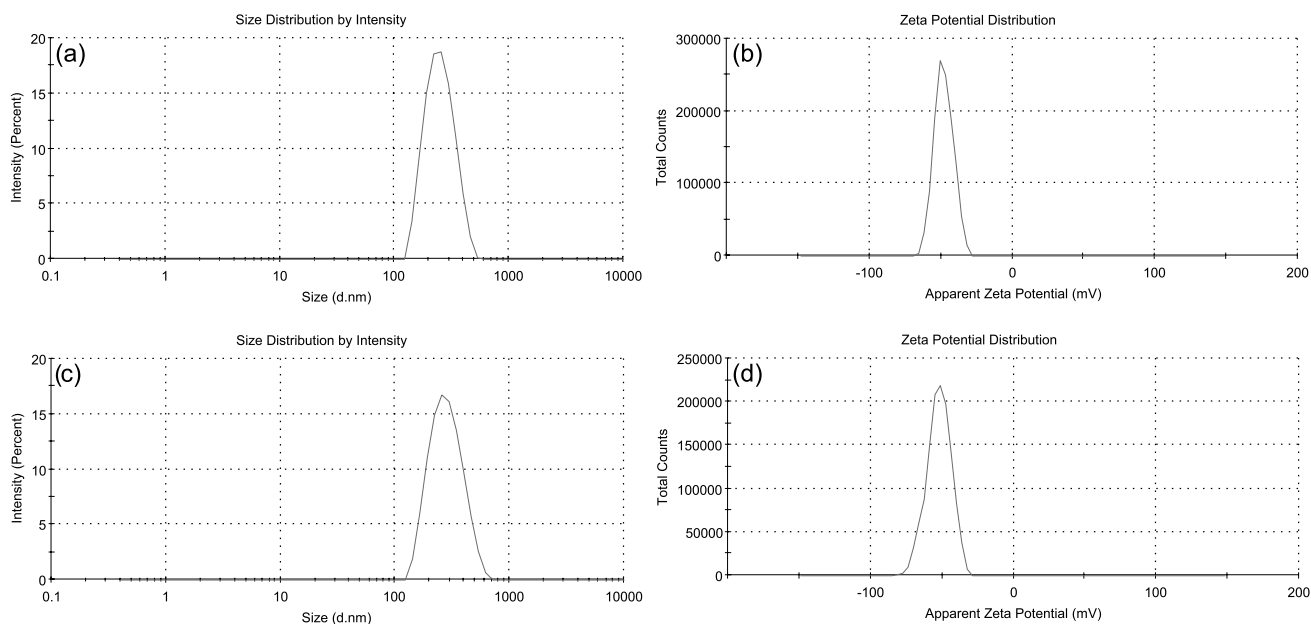
FF and FP nanoemulsions showed particle size values in the range of 189 and 211 nm, polydispersity index (PdI) of 0.105 and 0.118 and zeta potential of -36.5 and -43.4 mV, respectively, as shown in Table 2 and Figure 2.

Diameter values between 156.8 and 225.6 nm were obtained by Mazonde *et al.*³⁶ in nanoemulsions based on linseed oil with Span 20 and Tween 80 as surfactants. The medical applications of nanoparticles are strongly dependent on particle size. In most cases, this dependence is related to the requirements and characteristics of the biological systems studied.³⁷ The particle size is also related to the physical stability of the emulsions. The smaller the dispersed particles, the more stable the system is. On the other hand, the faster the particles increase in size, the more unstable the system becomes.³⁸ Cavazos-Garduño *et al.*³⁹ obtained nanoemulsions containing stable betulinic acid with particle size values close to 200 nm.

Table 2. Results from physicochemical characterization of unloaded and betulinic acid-loaded nanoemulsions

Formulation	Diameter / nm	PdI	Zeta potential / mV	Betulinic acid / ($\mu\text{g g}^{-1}$)
FF	189 ± 3	0.105 ± 0.003	-36.5 ± 1.2	1490 ± 2
FP	211 ± 4	0.118 ± 0.002	-43.4 ± 0.9	1477 ± 2
Control-FF	172 ± 5	0.111 ± 0.004	-32.1 ± 2.1	–
Control-FP	179 ± 2	0.104 ± 0.004	-39.7 ± 1.9	–

FF: nanoemulsion with only Pluronic F127 as surfactant; FP: nanoemulsion with Pluronic F127 and PGPR as surfactant; Control-FF: nanoemulsion FF betulinic acid free; Control-FP: nanoemulsion FP betulinic acid free; PdI: polydispersion index.

**Figure 2.** Size distribution by intensity and zeta potential. (a) and (b) FF nanoemulsion; (c) and (d) FP nanoemulsion.

The zeta potential values of the formulations FF and FP (-36.5 ± 1.2 and -43.4 ± 0.9 mV) were negative and favorable to stability according to Table 2. Zeta potential values greater than $+25$ mV or lower than -25 mV, indicate electrostatic stability, favoring repulsion between nanoparticles.⁴⁰ The negative surface charge can be attributed to the ionization of the carboxyl groups of fatty acids present in the composition of linseed oil. Nanoemulsions stabilized by polymers of high molecular weight and zeta potential values close to 20 mV are considered stable.⁴¹ The presence of Pluronic F127 in the composition of nanoemulsions promotes steric hindrance, allowing the process of coalescence due to its large molecular structure. For biological applications, steric stabilization is more advantageous than electrostatic stabilization since the stability of the particles is maintained even in the presence of existing charges.⁴²

The values of the polydispersion index (PdI) were also considered favorable for colloidal stability, with monodispersed distribution, as shown in Figure 2 and Table 2 with $\text{PdI} < 0.2$.⁴³ The (PdI) value is dimensionless and represents the distribution particle size. From the

polydispersity indices, a future phenomenon of colloidal instability of nanoemulsions can be predicted, in which particles with larger sizes encompass smaller particles until coalescence (phase separation), this phenomenon is called Ostwald ripening.

The concentration of betulinic acid in the nanoemulsions was 1490 ± 2 and 1477 ± 2 $\mu\text{g g}^{-1}$, corresponding to 99.33 and 98.46% of the nominal value of 1500 $\mu\text{g g}^{-1}$, respectively for FF and FP formulations, showing little loss of active during preparation from formulations.

The efficiency encapsulation (EE) obtained was greater than 99.99% for both formulations, considering the limit of quantification of the method. This high value is due to the intermolecular interaction between betulinic acid, the linseed oil components and the high hydrophobicity of betulinic acid.

Rheological assay

Understanding the rheology of a fluid is necessary for the functionality of the drug and for the use by the patient in

a pharmaceutical form suitable for the environment where it will be applied. Figures 3a and 3b shows the rheological properties of FF and FP nanoformulations.

No differences were observed in the flow behavior for the different formulations (FF and FP), which was identified as non-Newtonian flow, pseudoplastic type, as there is variation in viscosity with the increase in the shear rate. This rheological behavior was confirmed by the adjustment of the flow curves by the power law (equation 1), where it was possible to verify $n < 1$, typical of pseudoplastic fluids.

Adjusting to the power law model, the flow behavior index (f), consistency index (K) and determination coefficient (R^2) are obtained. The FF nanoemulsion with $K = 0.001242 \text{ Pa s}$, $f = 0.9894$, $R^2 = 0.9987$ and FP nanoemulsion with $K = 0.006517 \text{ Pa s}$, $f = 0.9094$, $R^2 = 0.9979$. The obtained curves reflect a non-Newtonian behavior. It is observed that the viscosity of the two formulations depends strongly on the shear rate up to 266 s^{-1} as shown in Figure 3b, which can be explained by the fact

that the forces existing between the particles at low shear rates are more pronounced than the hydrodynamic forces imposed by the shear. Wulff-Pérez *et al.*⁴⁴ observed in the rheological study of several nanoemulsion formulations that, as the shear rate increases, the hydrodynamic contribution prevails and the shear viscosity curves of the formulations get closer, as they have similar particle size. This fact was also observed in this work with the formulations FP and FF.

Storage stability and thermodynamic stability studies

The particle size results after 90 days (Figure 4) reveal an increase in size for the FF and FP formulations at the temperatures of 25 and 45 °C.

The sharpest increase was at 45 °C in which the FF formulation fluctuated from 189 to 253 nm ($p < 0.05$) and the FP formulation from 211 to 264 nm ($p < 0.05$). Nevertheless, even considering the observed variations in

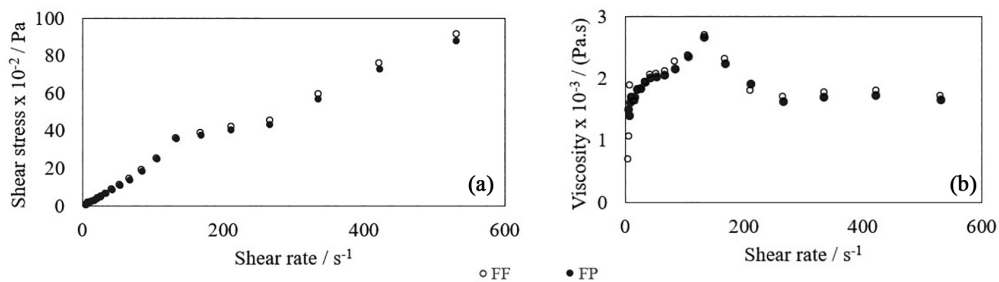


Figure 3. Stress (a) and viscosity (b) curves as a function of shear rate at 25 °C.

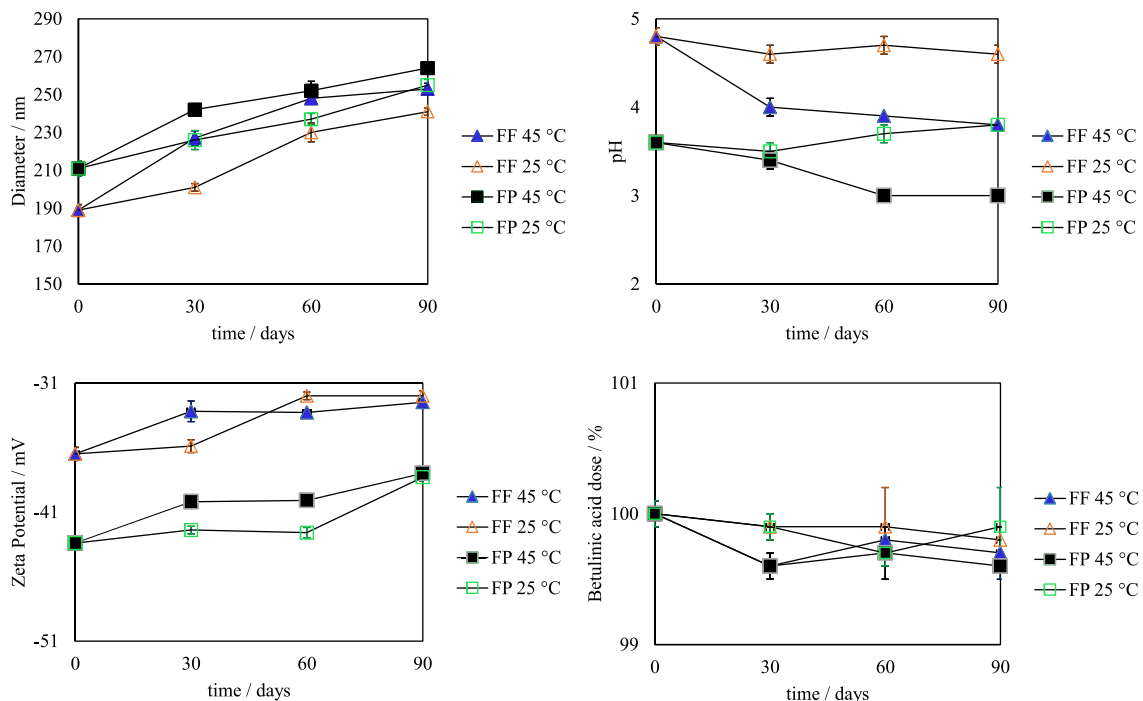


Figure 4. Droplet diameter, pH, zeta potential and betulinic acid dose variation during the storage stability assay.

size, zeta potential, pH and Pdl, the maximum reduction of the percentage of the initial value of betulinic acid was only -0.4% in the FP nanoemulsion at a temperature of $45\text{ }^{\circ}\text{C}$, leaving the final value of $99.6 \pm 0.1\%$ of the initial value of betulinic acid ($p < 0.05$). According to Brazilian legislation,⁴⁵ the reduction of less than 10% in the drug content in the accelerated stability tests allows for the drug a provisional shelf life of 12 months, but for definitive certainty of the shelf-life other criteria must be validated.

The electrostatic repulsion between the droplets provided by the zeta potential was sufficient to overcome the attractive forces and maintain the stability of the nanoemulsions for 90 days. Therefore, the combination of electrostatic and steric stabilization mechanisms caused by the presence of Pluronic F127 provided good colloidal stability for the proposed nanoemulsion system.

Thermodynamic tests are used to diagnose metastable formulations. Temperature (hot and cold cycles) and mechanical (centrifugation) stress conditions accelerate instability phenomena resulting from problems in the initial formulation. No formulation showed evidence of precipitation, phase separation, color change and creaming after thermodynamic tests and after the storage stability test.

Solubility, release and kinetic studies *in vitro*

In order to determine the sink condition, the solubility test was performed. The results are shown in Table 3, which presents the saturation values and the sink condition.

Table 3. Solubility test results

DMSO:PBS 7.4	Solubility BA / ($\mu\text{g g}^{-1}$)	Sink condition / ($\mu\text{g g}^{-1}$)
10:90	318	≤ 106
30:70	780	≤ 260

DMSO:PBS 7.4: dimethyl sulfoxide:phosphate-buffered saline pH 7.4; BA: betulinic acid.

Since the amount of betulinic acid in 1 g of nanoemulsion is $1500\text{ }\mu\text{g}$ and if all this amount is released in 11.7 mL of the receiving medium, there is a maximum concentration of $135.5\text{ }\mu\text{g g}^{-1}$ if 100% of the active is released. However, the saturation concentration of the DMSO:phosphate buffered ratio (PBS, pH = 7.4) 30:70 is $780\text{ }\mu\text{g g}^{-1}$ and 1/3 of this saturation is the sink condition which corresponds to $260\text{ }\mu\text{g g}^{-1}$, that is, greater than the maximum concentration to be achieved in the release test. The approved receiving medium for the sink condition is DMSO:phosphate buffered (PBS, pH = 7.4) 30:70.

The *in vitro* release profiles of betulinic acid from the linseed oil nanoemulsion containing PGPR and Pluronic F127 as stabilizers are shown in Figure 5.

The amount of betulinic acid (BA) contained in the nanoemulsions was $1500\text{ }\mu\text{g g}^{-1}$. In 48 h the FF formulation released 41.13% and the FP formulation released 38.15% corresponding to 619.95 and 572.25 μg of betulinic acid, respectively.

The Higuchi and Korsmeyer-Peppas models were tested as shown in Table 4.

After linearizing the Higuchi and Korsmeyer-Peppas equations, the R^2 value was determined, obtaining the values closest to 1 for the Korsmeyer-Peppas model for the two formulations (0.9904 and 0.9931). For the Korsmeyer-Peppas model, the value of the exponent n that corresponds to the slope value after linearization and the value of the constant k that corresponds to 10^b , where b is the linear coefficient of the linearized equation, were also determined.

The FF formulation, containing only Pluronic F127 polymer as a surfactant, showed higher values of K and J and lower lag time for the start of release according to the statistical analysis. This fact can be explained by the greater amount of Pluronic F127 in relation to the FP formulation, since this polymer has a higher HLB value than PGPR, interacting better with aqueous solutions. The value of n of the Korsmeyer-Peppas equation for the FF

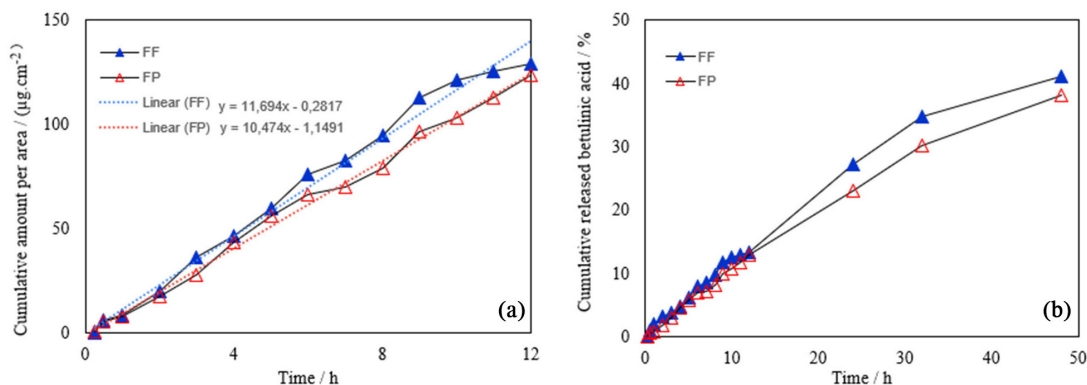


Figure 5. *In vitro* release profile of betulinic acid: (a) cumulative amount released per area in 12 h and (b) cumulative percentage released in 48 h.

Table 4. Kinetic parameters of release and linearity of the tested models

Formulation	Korsmeyer-Peppas model			Higuchi model	J / ($\mu\text{g cm}^{-2} \text{ h}^{-1}$)	Lag time / h
	k	n	R ²	R ²		
FF	0.0162	0.8621	0.9904	0.9727	11.694	0.024
FP	0.0086	1.1088	0.9931	0.9679	10.474	0.109

FF: nanoemulsion with only Pluronic F127 as surfactant; FP: nanoemulsion with Pluronic F127 and PGPR as surfactant; R²: determination coefficient; k: constant related to the structural and geometric characteristics of the dosage form; n: release exponent; J: state flux.

formulation presented a value of 0.8621 and for the FP formulation it was 1.1088, identifying the Super Case II Transport mechanism. According to Korsmeyer-Peppas, for particles with a spherical geometric shape, values of n greater than 0.85 refer to the Super Case II Transport mechanism. In this mechanism, there is a rapid penetration of the solvent and relaxation of the polymeric chains, and, in this way, the drug is released.³⁰

The kinetics of drug release from a nanoemulsion formulation is extremely relevant in the development of drug delivery systems. An *in vitro* release profile reveals important information about the structure and behavior of the formulation components, the interactions between the drug and the encapsulating system, the influence on the rate and mechanism of drug release.⁴⁶ This indicates slow release of betulinic acid due to its low solubility in the dissolution medium.⁴⁷ For comparison purposes with our system, we did not find a release test for betulinic acid nanoemulsions. However, there are some studies with other similar triterpenes such as ursolic acid and oleanolic acid. The ursolic acid and oleanolic acid were released from the castor oil, labrasol and transcuto-P nanoemulsions after 75 h in the percentages of 44.40 to 47.22%.⁴⁸

MTT assay

The results obtained from the IC₅₀ values are described in Table 5 and Figure 6.

Table 5. Cytotoxic activity after 72 h incubation

Sample	SNB-19		NCI-H460		HCT-116		L-929	
	IC ₅₀ (SD) / μM	IC ₅₀ / ($\mu\text{g mL}^{-1}$)	IC ₅₀ (SD) / μM	IC ₅₀ / ($\mu\text{g mL}^{-1}$)	IC ₅₀ (SD) / μM	IC ₅₀ / ($\mu\text{g mL}^{-1}$)	IC ₅₀ (SD) / μM	IC ₅₀ / ($\mu\text{g mL}^{-1}$)
BA	3.44 (2.90-4.05)	1.57	1.30 (1.03-1.54)	0.60	3.42 (2.75-4.20)	1.56	8.70 (6.02-12.15)	3.96
BAF	> 11,00		> 11,00		> 11,00		> 11,00	
Control-FP	8.80 (6.80-11.50)	4.04	> 16.50		4.90 (3.90-6.10)	2.21	> 16.50	
Control-FF	7.12 (5.20-9.80)	3.25	8.00 (5.90-11.00)	3.66	5.70 (4.30-7.50)	2.60	> 16.50	
FF	5.80 (4.08-8.28)	2.65	5.60 (5.00-6.30)	2.54	3.20 (2.60-3.90)	1.46	> 16.50	
FP	7.30 (6.20-8.50)	3.32	11.50 (9.00-14.85)	15.27	3.70 (3.00-4.70)	1.71	> 16.50	

SD: standard deviation; BA: betulinic acid; BAF: betulinic acid mixed in linseed oil; FP: FP nanoemulsion; FF: FF nanoemulsion; Control-FP: FP nanoemulsion drug unloaded and Control-FF: FF nanoemulsion drug unloaded; HCT-116 colorectal carcinoma; SNB-19: glioblastoma; NCI-H460: lung carcinoma; L-929: normal fibroblasts cells; IC₅₀: 50% inhibitory concentration.

The selectivity index consists of the ratio between the 50% cytotoxic concentrations for non-tumor cells and the IC₅₀ of tumor cells. This index indicates how much a substance is less toxic to non-tumor cells than to tumor cells, and this proportion is considered good when the index is equal to or greater than 2.⁴⁹ This value is considered significant because it means that the component is twice as much active against the tumor cell line than the non-tumor cell line.

When evaluating the highest concentration tested of betulinic acid in nanoemulsions (16.5 μM), it did not presented cytotoxicity, since the conversion of MTT into formazan occurred in similar proportion to negative control cells, leading to the conclusion that the cells remained viable after treatment with the nanoemulsions. However, when the same non tumoral cell line was incubated with betulinic acid in the free form, it presented IC₅₀ 8.7 μM , showing that the free substance promoted toxicity non-tumor cell line. These findings indicate that the nanoemulsions are able to kill the tumor cells without causing quantitative damage in the non-tumoral cells evaluated in the present study. This same behavior was observed with betulinic acid in nanotubes, which showed that the IC₅₀ results of nanostructured betulinic acid suggest a reduction in toxicity for normal cells and, consequently, a reduction in side effects.⁵⁰ This fact can be explained by the release of betulinic acid in nanoemulsions slowly exposing the cells to a gradual drug action and with small variations for a longer

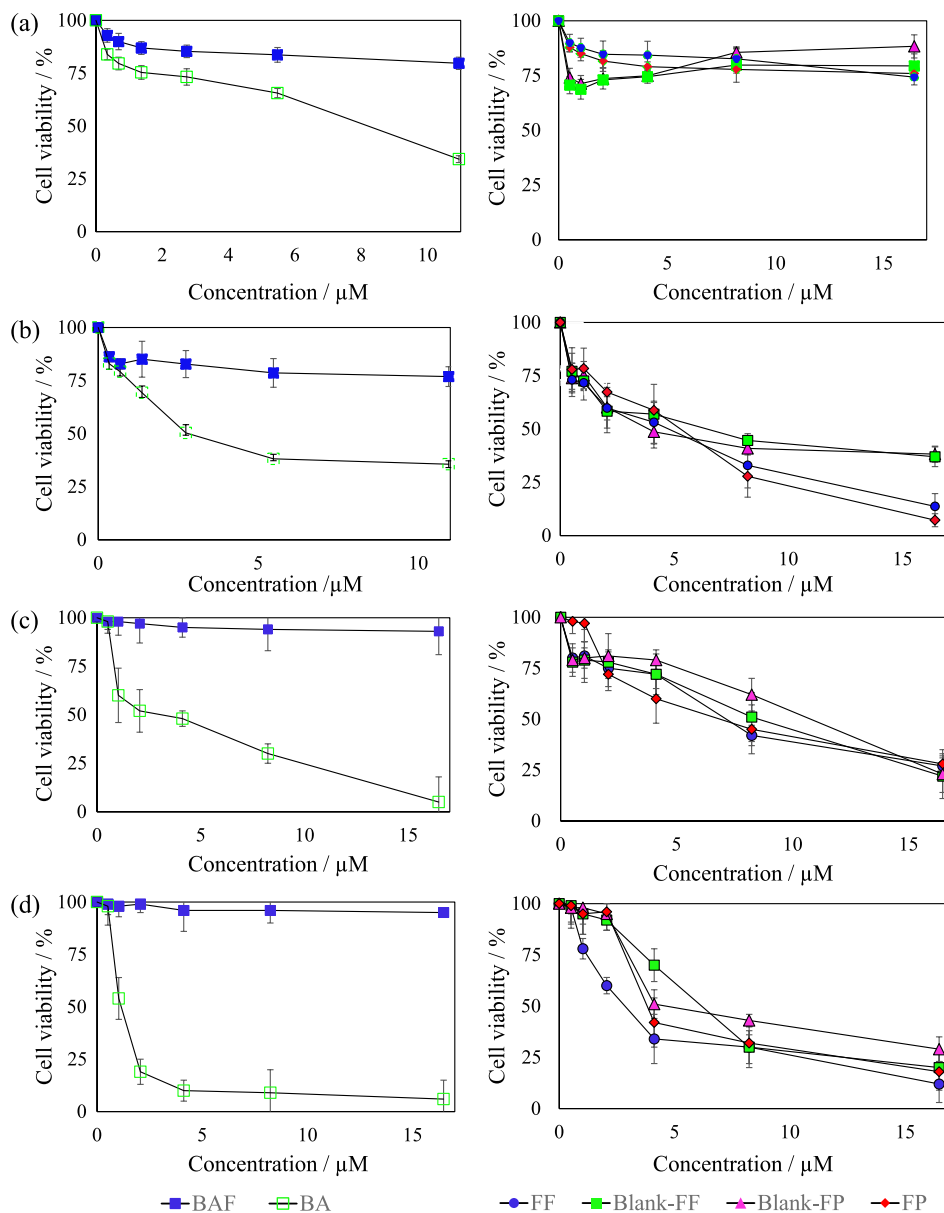


Figure 6. Cell viability in function of concentration of drug delivery nanoemulsions (FF and FP), control nanoemulsions (blank-FF and blank-FP), betulinic acid (BA) and oil-betulinic acid (BAF). (a) L-929 (normal fibroblasts) cells, (b) HCT-116 (colorectal carcinoma) cells, (c) SNB-19 (glioblastoma) cells and (d) NCI-H460 (lung carcinoma) cells.

time. Victor *et al.*⁵¹ presented IC_{50} at 72 h for $1.73 \mu\text{g mL}^{-1}$ pure betulinic acid against HCT-116 cells, that is, similar to that obtained in this work.

In view of the results presented, it was observed that free betulinic acid (BA) showed high cytotoxic activity in HCT-116 (IC_{50} $3.42 \mu\text{M}$), SNB-19 (IC_{50} $3.44 \mu\text{M}$) and NCI-H460 (IC_{50} $1.30 \mu\text{M}$) while betulinic acid mixed with oil (not nanoemulsified) BAF did not show cytotoxicity at the maximum concentration tested ($11 \mu\text{M}$).

It was observed that betulinic acid solubilized in oil did not present cytotoxic activity in all strains, that is, linseed oil and betulinic acid act only in nanoemulsified form. There are reports that in multidrug-resistant tumors,

Pluronic is able to act on tumor cells, increasing their permeability to antineoplastic drugs and can induce changes in various cellular functions, including gene expression, mitochondrial breathing and ATP synthesis, increasing the effectiveness of treatment.⁵² Therefore, it is possible that the action is related to the polymer Pluronic F127 or to the small size of the oily particles.

Only in HCT-116 cells there was a significant difference ($p < 0.05$) between the IC_{50} results of the control of the FF nanoemulsion and the FF nanoemulsion containing betulinic acid, and it can be affirmed that the FF nanoemulsion containing betulinic acid showed better antitumor activity *in vitro* than the control FF formulation (without betulinic

acid). In these same cells, the FF and FP nanoemulsions showed no statistically significant differences ($p > 0.05$) in relation to free betulinic acid. However, in SNB-119 and NCI-H460 cells, nanoemulsions with betulinic acid showed lower cytotoxic activity ($p < 0.05$) than free betulinic acid.

Free betulinic acid proved to be more cytotoxic ($p < 0.05$) against NCI-H460 cells (IC_{50} 1.3 μM) compared with samples of nanoemulsions containing betulinic acid (IC_{50} 5.6 and 11.5 μM) and the mixture of betulinic acid with linseed oil ($IC_{50} > 11 \mu\text{M}$). It was also observed that the free betulinic acid was more selective than the nanoemulsions containing the drug encapsulated in linseed oil and only the surfactant F127 and water against these NCI-H460 cells. Studies by Zhan *et al.*⁵³ evaluating an antiproliferative activity in paclitaxel-resistant NCI-H460 cells (lung carcinoma) by the MTT assay revealed that betulinic acid exhibited an IC_{50} of 50 μM in 48 h and that it was concentration dependent. However, it was not found in the literature, the IC_{50} in H460 cells for betulinic acid in 72 h so that it could be compared with our study that found a value of 1.3 μM in 72 h.

It is worth mentioning that an important factor that can influence cytotoxic activity of nanostructured formulations is particle size. Studies by Ting *et al.*⁵⁴ verified the influence of 5-DT (5-dimethyltangeretin) delivery systems on the growth of cancer cells HCT-116 with 24 h of treatment and together with the results of MTT testing and microscopic observation, emulsion-based systems have proven to be effective and efficient to increase the anti-proliferative cancer-related properties of tangeretin *in vitro*.

Conclusions

The nanoemulsions synthesized in this work showed characteristics of colloidal stability. The MTT test revealed preliminary *in vitro* cytotoxic activity against HCT-116 (colorectal cancer), NCI-H460 and SNB-19 cells. In addition, nanoemulsions formulated with encapsulated betulinic acid were more advantageous than free betulinic acid in relation to colorectal carcinoma cells in preliminary cytotoxic selectivity tests, as they did not show cytotoxic potential against non-tumor fibroblast cells, unlike pure betulinic acid. The proposed nanosystems also showed a kinetic profile of *in vitro* release in a controlled manner. Therefore, the proposed nanoemulsions functioned successfully as hydrophobic betulinic acid carriers, representing a promising therapeutic agent when strategically stabilized with Pluronic F127. As part of our continuous improvement, *in vivo* trials are underway for the incorporation of this nanoemulsion into hydrophilic matrices of rectal suppositories for colorectal carcinoma.

Acknowledgments

This study was partially supported by the Coordenação de Aperfeiçoamento de Pessoal de Nível Superior - Brasil (CAPES) - Finance Code 001 (PROEX 23038.000509/2020-82) and Conselho Nacional de Desenvolvimento Científico e Tecnológico (CNPq). The authors thank Central Analítica-UFC/CT-INFRA/MCTI-SISNANO/CAPES for the support. The corresponding author thanks CNPq for the research grant (N.M.P.S.R No. 309795/2021-4).

Author Contributions

Louhana M. Rebouças was responsible for investigation, formal analysis, writing original draft and editing; Nilce V. Gramosa for project administration; Fátima de Cássia Evangelista for investigation; Alexandre C. C. Sousa for investigation and writing-review; Tamara G. de Araújo for investigation; Cláudia do Ó Pessoa for investigation and software; Rinaldo S. Araújo for conceptualization; Emília Maria A. Santos for writing original draft; Nágila Maria P. S. Ricardo for project administration, writing-review and funding acquisition.

References

1. Ashaolu, T. J.; *Environ. Chem. Lett.* **2021**, *19*, 3381. [Crossref]
2. Qu, Y.; Li, A.; Ma, L.; Iqbal, S.; Sun, X.; Ma, W.; Li, C.; Zheng, D.; Xu, Z.; Zhao, Z.; Ma, D.; *Int. J. Pharm.* **2021**, *597*, 120250. [Crossref]
3. Fardous, J.; Omoso, Y.; Joshi, A.; Yoshida, K.; Patwary, M. K. A.; Ono, F.; Ijima, H.; *Mater. Sci. Eng., C* **2021**, *124*, 112076. [Crossref]
4. Ansari, M. J.; Alnakhli, M.; Al-Otaibi, T.; Al Meanazel, O.; Anwer, M. K.; Ahmed, M. M.; Alshahrani, S. M.; Alshetaili, A.; Aldawsari, M. F.; Alalawi, A. S.; Alanazi, A. Z.; Zahrani, M. A.; Ahmad, N.; *J. Drug Delivery Sci. Technol.* **2021**, *61*, 102204. [Crossref]
5. Sousa, A. C. C.; Romo, A. I. B.; Almeida, R. R.; Silva, C. C.; Fechine, L. M. U.; Brito, H. A.; Freire, R. M.; Pinheiro, D. P.; Larissa, M.; Ricardo, M. P. S.; Silva, R.; Pessoa, O. D. L.; Denardin, J. C.; Pessoa, C.; *Carbohydr. Polym.* **2021**, *264*, 118017. [Crossref]
6. Zoabi, A.; Touitou, E.; Margulis, K.; *Colloids Interfaces* **2021**, *5*, 18. [Crossref]
7. Pisha, E.; Chai, H.; Lee, I. S.; Chagwedera, T. E.; Farnsworth, N. R.; Cordell, G. A.; Beecher, C. W. W.; Fong, H. H. S.; Kinghorn, A. D.; Brown, D. M.; Wani, M. C.; Wall, M. E.; Hieken, T. J.; Gupta, T. K. D.; Pezzuto, J. M.; *Nat. Med.* **1995**, *1*, 1046. [Crossref]
8. Coricovac, D.; Dehelean, C. A.; Pinzaru, I.; Mioc, A.; Aburel, O. M.; Macasoi, I.; Draghici, G. A.; Petean, C.; Soica, C.; Boruga, M.; Vlaicu, B.; Muntean, M. D.; *Int. J. Mol. Sci.* **2021**, *22*, 4870. [Crossref]

9. Park, C.; Jeong, J. W.; Han, M. H.; Lee, H.; Kim, G. Y.; Jin, S.; Park, J. H.; Kwon, H. J.; Kim, B. W.; Choi, Y. H.; *Anim. Cells Syst.* **2021**, *25*, 119. [Crossref]
10. Laszczyk, M. N.; *Planta Med.* **2009**, *75*, 1549. [Crossref]
11. Zhang, D. M.; Xu, H. G.; Wang, L.; Li, Y. J.; Sun, P. H.; Wu, X. M.; Wang, G. J.; Chen, W. M.; Ye, W. C.; *Med. Res. Rev.* **2015**, *35*, 1127. [Crossref]
12. Kim, S. Y.; Hwangbo, H.; Kim, M. Y.; Ji, S. Y.; Kim, D. H.; Lee, H.; Kim, G. Y.; Moon, S. K.; Leem, S. H.; Yun, S. J.; Kim, W. J.; Cheong, J. H.; Park, C.; Choi, Y. H.; *Molecules* **2021**, *26*, 1381. [Crossref]
13. Feng, J.; Shi, Y.; Yu, Q.; Sun, C.; Yang, G.; *Colloids Surf., A* **2016**, *497*, 286. [Crossref]
14. Lucas, E. A.; Wild, R. D.; Hammond, L. J.; Khalil, D. A.; Juma, S.; Daggy, B. P.; Stoecker, B. J.; Arjmandi, B. H.; *J. Clin. Endocrinol. Metab.* **2002**, *87*, 1527. [Crossref]
15. Fukui, M.; Kang, K. S.; Okada, K.; Zhu, B. T.; *J. Cell. Biochem.* **2013**, *114*, 192. [Crossref]
16. Redhead, H. M.; Davis, S. S.; Illum, L.; *J. Controlled Release* **2001**, *70*, 353. [Crossref]
17. Lin, Y.; He, X.; Zhou, D.; Li, L.; Sun, J.; Jiang, X.; *RSC Adv.* **2018**, *8*, 23768. [Crossref]
18. Guan, Y.; Huang, J.; Zuo, L.; Xu, J.; Si, L.; Qiu, J.; Li, G.; *Arch. Pharmacol. Res.* **2011**, *34*, 1719. [Crossref]
19. Dehelean, C. A.; Feflea, S.; Ganta, S.; Amiji, M.; *J. Biomed. Nanotechnol.* **2011**, *7*, 317. [Crossref]
20. Agame-Lagunes, B.; Grube-Pagola, P.; García-Varela, R.; Alexander-Aguilera, A.; García, H. S.; *Pharmaceutics* **2021**, *13*, 509. [Crossref]
21. *Mass Spectral Research Program*, version 2.0; NIST, USA, 2008.
22. Taralkar, S. V.; Chattopadhyay, S.; *J. Anal. Bioanal. Tech.* **2012**, *3*, 1000134. [Crossref]
23. Kumari, S.; Kumaraswamy, R. V.; Choudhary, R. C.; Sharma, S. S.; Pal, A.; Raliya, R.; Biswas, P.; Saharan, V.; *Sci. Rep.* **2018**, *8*, 6650. [Crossref]
24. Yu, S.; Tan, G.; Liu, D.; Yang, X.; Pan, W.; *RSC Adv.* **2017**, *7*, 16668. [Crossref]
25. *TA Instruments Operating software*; Rheology Advantage Instrument Control AR, TA Instruments, USA, 2000.
26. Liu, Y.; Liu, L.; Wang, Y.; Zhu, G.; Tan, W.; *RSC Adv.* **2016**, *6*, 102938. [Crossref]
27. Md, S.; Alhakamy, N.; Aldawsari, H.; Kotta, S.; Ahmad, J.; Akhter, S.; Alam, M.; Khan, M.; Awan, Z.; Sivakumar, P.; *J. Chem.* **2020**, 2020, ID 4071818. [Crossref]
28. Weng, J.; Tong, H. H.; Chow, S. F.; *Pharmaceutics* **2020**, *12*, 732. [Crossref]
29. Liu, P.; de Wulf, O.; Laru, J.; Heikkilä, T.; van Veen, B.; Kiesvaara, J.; Hirvonen, J.; Peltonen, L.; Laaksonen, T.; *AAPS PharmSciTech* **2013**, *14*, 748. [Crossref]
30. Korsmeyer, R. W.; Gurny, R.; Doelker, E.; Buri, P.; Peppas, N. A.; *Int. J. Pharm.* **1983**, *15*, 25. [Crossref]
31. Higuchi, T.; *J. Pharm. Sci.* **1963**, *52*, 1145. [Crossref]
32. Macheras, P.; Iliadis, A.; *Modeling in Biopharmaceutics, Pharmacokinetics and Pharmacodynamics: Homogeneous and Heterogeneous Approaches*, vol. 29; Springer: New York, USA, 2006, p. 57. [Crossref]
33. Ye, Q.; Wang, X.; Jin, M.; Wang, M.; Hu, Y.; Yu, S.; Yang, Y.; Yang, J.; Cai, J.; *World J. Surg. Oncol.* **2018**, *16*, 240. [Crossref]
34. *GraphPad Prism*, version 5.00; GraphPad Software, Inc.; USA, 2008.
35. Chauhan, R.; Chester, K.; Khan, Y.; Tamboli, E. T.; Ahmad, S.; *J. Pharm. BioAllied Sci.* **2015**, *7*, 284. [Crossref]
36. Mazonde, P.; Khamanga, S. M. M.; Walker, R. B.; *Pharmaceutics* **2020**, *12*, 797. [Crossref]
37. Rahn-Chique, K.; Urbina-Villalba, G.; *J. Dispersion Sci. Technol.* **2017**, *38*, 167. [Crossref]
38. Ursica, L.; Tita, D.; Palici, I.; Tita, B.; Vlaia, V.; *J. Pharm. Biomed. Anal.* **2005**, *37*, 931. [Crossref]
39. Cavazos-Garduño, A.; Ochoa Flores, A. A.; Serrano-Niño, J. C.; Beristain, C. I.; García, H. S.; *Rev. Mex. Ing. Quim.* **2014**, *13*, 689. [Link]
40. Elemike, E. E.; Onwudiwe, D. C.; Nundkumar, N.; Singh, M.; Iyekowa, O.; *Mater. Lett.* **2019**, *243*, 148. [Crossref]
41. Honary, S.; Zahir, F.; *Trop. J. Pharm. Res.* **2013**, *12*, 265. [Crossref]
42. Kim, T.; Lee, C. H.; Joo, S. W.; Lee, K.; *J. Colloid Interface Sci.* **2008**, *318*, 238. [Crossref]
43. Du, Z.; Wang, C.; Tai, X.; Wang, G.; Liu, X.; *ACS Sustainable Chem. Eng.* **2016**, *4*, 983. [Crossref]
44. Wulff-Pérez, M.; Martín-Rodríguez, A.; Gálvez-Ruiz, M. J.; de Vicente, J.; *Colloid Polym. Sci.* **2013**, *291*, 709. [Crossref]
45. Agência Nacional de Vigilância Sanitária (ANVISA); Resolução da Diretoria Colegiada (RDC) No. 318, de 06 de novembro de 2019, *Estabelece os Critérios para a Realização de Estudos de Estabilidade de Insumos Farmacêuticos Ativos e Medicamentos, Exceto Biológicos*; Diário Oficial da União (DOU), Brasília, No. 216, de 07/11/2019, p. 97. [Link] accessed in December 2021
46. Hua, S.; *Int. J. Nanomed.* **2014**, *9*, 735. [Crossref]
47. Monteiro, L. M.; Lione, V. F.; do Carmo, F. A.; do Amaral, L. H.; da Silva, J. H.; Nasciutti, L. E.; Rodrigues, C. R.; Castro, H. C.; de Sousa, V. P.; Cabral, L. M.; *Int. J. Nanomed.* **2012**, *7*, 5175. [Crossref]
48. Alvarado, H. L.; Abrego, G.; Souto, E. B.; Garduño-Ramirez, M. L.; Clares, B.; García, M. L.; Calpena, A. C.; *Colloids Surf., B* **2015**, *130*, 40. [Crossref]
49. Suffness, M.; Pezzuto, J. M.; *Methods in Plant Biochemistry: Assays for Bioactivity*, vol. 6; Hostettmann, K., ed.; Academic Press: London, UK, 1990, p. 376.
50. Tan, J. M.; Karthivashan, G.; Arulselvan, P.; Fakurazi, S.; Hussein, M. Z.; *Drug Des., Dev. Ther.* **2014**, *8*, 2333. [Crossref]

51. Victor, M. M.; David, J. M.; Sakukuma, M. C. K.; Costa-Lotufo, L. V.; Moura, A. F.; Araújo, A. J.; *An. Acad. Bras. Cienc.* **2017**, *89*, 1369. [Crossref]
52. Devi, D. R.; Sandhya, P.; Hari, B. N. V.; *J. Pharm. Sci. Res.* **2013**, *5*, 159. [Link]
53. Zhan, X. K.; Li, J. L.; Zhang, S.; Xing, P. Y.; Xia, M. F.; *Oncol. Lett.* **2018**, *16*, 3628. [Crossref]
54. Ting, Y.; Chiou, Y. S.; Pan, M. H.; Ho, C. T.; Huang, Q.; *J. Funct. Foods* **2015**, *15*, 264. [Crossref]

Submitted: January 25, 2022
Published online: April 14, 2022

